

Electron Spectral Functions of Reconstructed Quantum Hall Edges

A. Melikidze and Kun Yang

National High Magnetic Field Laboratory, 1800 E. Paul Dirac Dr., Tallahassee, FL 32310

(Dated: November 7, 2003)

During the reconstruction of the edge of a quantum Hall liquid, Coulomb interaction energy is lowered through the change in the structure of the edge. We use theory developed earlier by one of the authors [K. Yang, Phys. Rev. Lett. **91**, 036802 (2003)] to calculate the electron spectral functions of a reconstructed edge, and study the consequences of the edge reconstruction for the momentum-resolved tunneling into the edge. It is found that additional excitation modes that appear after the reconstruction produce distinct features in the energy and momentum dependence of the spectral function, which can be used to detect the presence of edge reconstruction.

PACS numbers: 73.43.-f, 71.10.Pm

The paradigm of the Quantum Hall effect (QHE) edge physics is based on an argument due to Wen,¹ according to which the low-energy edge excitations are described by a chiral Luttinger liquid (CLL) theory. One attractive feature of this theory is that due to the chirality, the interaction parameter of the CLL is often tied to the robust topological properties of the bulk and is independent of the details of electron interaction and edge confining potential; studying the physics at the edge thus offers an important probe of the bulk physics. It turns out, however, that the CLL ground state may not always be stable.^{2,3} On the microscopic level, the instability is driven by Coulomb interactions and leads to the change of the structure of the edge. This effect has been termed “edge reconstruction”. One of its manifestations is the appearance of new low-energy excitations of the edge not present in the original CLL theory.

Based on the insight from numerical studies of the edge reconstruction,^{4,5} a field-theoretic description of the effect has been proposed by one of us.⁶ Remarkably, it provides an explicit expression for the electron operator in terms of the fields that describe the low-energy edge excitations after the reconstruction. This allows one to calculate many observable quantities. In this paper, we describe the calculation of the spectral function of the electron in the reconstructed edge. This function can be probed in tunneling experiments where the electron’s momentum parallel to the edge is conserved (the so-called momentum-resolved tunneling). Experiments of this kind are currently being performed.^{7,8} It has also been proposed that momentum-resolved tunneling may be used to detect the multiple branches of edge excitations of hierarchy states.⁹

Our results show that the appearance of the new edge excitations after the reconstruction modifies the electron spectral function qualitatively. It leads to the redistribution of the spectral weight away from the peak corresponding to the original edge mode, and produces singularities corresponding to the new edge modes. For simplicity we have focused on the principal Laughlin sequence, although generalization to the hierarchy states should be straightforward. We also propose a particular experimental setup that involves momentum-resolved

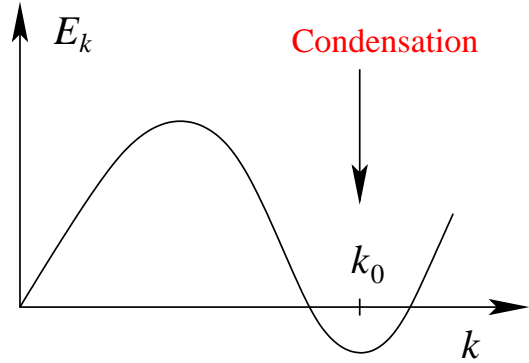


FIG. 1: The spectrum of the edge excitations after the reconstruction has a minimum below 0. Excitations with momenta near k_0 are condensed.

electron tunneling which is ideal for detecting possible edge reconstruction.

Previous numerical studies⁵ have suggested that the phenomenon of edge reconstruction can be understood as an instability of the original edge mode described by the CLL theory. This instability occurs as a result of increasing curvature of the edge spectrum as the edge confining potential softens. The spectrum curves down at high values of momenta until it touches zero at the transition point (see Fig. 1). This signals an instability of the ground state as the edge excitations begin to condense at finite momentum k_0 . Such condensation implies the appearance of a bump in the electron density localized in real space at $y_0 = l^2 k_0$, where y_0 is the coordinate normal to the edge and l is the magnetic length. These condensed excitations form a superfluid (with power-law correlation) which possesses a neutral “sound” mode that can propagate in both directions.

Following Ref. 6, we introduce two slowly varying fields ϕ_1 and φ which describe the original charged edge mode and the pair of the two new neutral modes, respectively. The total action of the reconstructed edge of the FQHE

at filling fraction $\nu = 1/m$ is: $S = S_1 + S_\varphi + S_{\text{int}}$, where

$$S_1 = \frac{m}{4\pi} \int dt dx [\partial_t \phi_1 \partial_x \phi_1 - v(\partial_x \phi_1)^2], \quad (1)$$

$$S_\varphi = \frac{K_1}{2} \int dt dx \left[\frac{1}{v_\varphi} (\partial_t \varphi)^2 - v_\varphi (\partial_x \varphi)^2 \right], \quad (2)$$

$$S_{\text{int}} = -K_2 \int dt dx (\partial_t \varphi)(\partial_x \phi_1). \quad (3)$$

Here, S_1 is the action of the original chiral charged mode with velocity v , S_φ is the action of the new neutral modes with velocities v_φ , S_{int} describes the interaction between them. The theory, developed in Ref. 6, predicts: $K_1 \sim K_2 \sim 1$, $v \gg v_\varphi$. The latter inequality comes from the fact that the Coulomb interaction boosts the velocity of the charged mode, but not those of neutral ones.

The action in Eqs. (1,2,3) describes the simplest situation where edge excitation condensed in the vicinity of a single point k_0 . Such condensation may also occur at multiple points, producing a set of pairs of additional neutral modes. The action in that case is a straightforward extension of Eqs. (2,3). We shall comment on the effect of such multiple edge reconstruction below.

The theory⁶ also provides an explicit expression for the electron operator:

$$\Psi = \exp \{ im\phi_1 + \rho \cos(k_0 x + \varphi) \}. \quad (4)$$

It has two parts: The first part contains ϕ_1 and describes an electron as being made up of the excitations of the original chiral edge mode. The second part contains φ and corresponds to the excitation of the neutral modes. The constant ρ is proportional to the density of the new condensate and thus rises from zero at the reconstruction transition.

Our goal is to calculate the electron spectral function. We begin by evaluating the Green's function in real space and imaginary-time representation: $g(x, \tau) = -i\langle \Psi(0, 0)\Psi(x, \tau) \rangle$. To this end, we write:

$$\Psi = e^{im\phi_1} \sum_{n=-\infty}^{\infty} c_n e^{in(k_0 x + \varphi)}, \quad (5)$$

In the long wave length limit, the dominant contribution to $g(x, \tau)$ will come from the term with $n = 0$ in the above series. Therefore, we only retain this term in what follows; the effect of the omitted terms will be commented upon in the discussion. Since the action of system is Gaussian, the evaluation of the Green's function is now straightforward. The expressions turn out quite cumbersome, but one may exploit the limits $v_\varphi \ll 1$, $x, \tau \rightarrow \infty$ to obtain:

$$g(x, \tau) \propto \prod_{i=1}^3 \frac{1}{(x + iv_i \tau)^{\alpha_i}}. \quad (6)$$

Here v_1, v_2 and v_3 are the velocities of the three modes: $v_1 \approx v(1 - 2\beta)$, $v_{2,3} \approx \pm v_\varphi(1 + \beta)$, where $\beta =$

$(\pi K_2^2/mK_1)(v_\varphi/v)$ is small. To second order in v_φ/v , the exponents are: $\alpha_1 \approx m$, $\alpha_{2,3} \approx (4\pi K_2^2/K_1)(v_\varphi/v)^2$. The sum of these three exponents describes local electron tunneling into the reconstructed edge and has been obtained earlier.⁶ Note also, that the "velocity conservation law", $\sum v_i = v$, derived in¹⁰ for a similar model, is not satisfied in our case due to slightly different interaction term S_{int} .

Next, one encounters a complication: the expression for the Green's function Eq. (6) is, in general, not single-valued. Therefore, the analytic continuation to the real time, needed to find the spectral function, is ambiguous and depends on the choice of branch cuts. A way around this difficulty was found in Ref.¹¹ for a similar problem, where an elegant trick was used to make the analytic continuation. However, this trick cannot be used in the present case because it fails for the values of the exponents α_i that appear in our problem. We shall use a different approach.

Notice that the Green's function in Eq. (6) is a product of three factors, each having a singularity corresponding to one of the three propagating modes after the reconstruction. The Green's function thus has the form:

$$G = g_1 g_2 g_3, \quad (7)$$

where g_i are (fictitious) Green's functions corresponding to the three modes. But each of these three Green's functions has a form identical to the electron Green's function of the original (unreconstructed) edge, the only variation between the three being the signs and absolute values of the velocities v_i of the edge modes and the edge exponents α_i . This allows us to write the electron spectral function as a convolution:

$$A(\Omega, Q) = \int \prod_{i=1}^3 A_i(\omega_i, q_i) \left[\prod_{i=1}^3 \theta(\omega_i) + \prod_{i=1}^3 \theta(-\omega_i) \right] \\ \times \delta(\Omega - \sum_{i=1}^3 \omega_i) \delta(Q - \sum_{i=1}^3 q_i) \prod_{i=1}^3 d\omega_i dq_i, \quad (8)$$

where $A_i(\omega, q) \propto |q|^{\alpha_i-1} \delta(\omega - v_i q)$ are the spectral functions corresponding to the Green's functions g_i . A typical plot of the spectral function is shown in Fig. 2. As a result of edge reconstruction, some of the spectral weight is shifted away from the original δ -function singularity at $\omega = vq$ (its new position $v_1 q$ is itself slightly renormalized). An extra pair of singularities appear at $\omega = v_{2,3} q$; these singularities correspond to the new neutral modes. An important feature of the spectral function is a finite amount of weight at $\omega < 0$. This is possible only due to the fact that, after the reconstruction, an excitation mode appears that propagates in the direction opposite to the direction of the original edge mode.

We now turn to the question of the possibility of experimental observation of the new features that appear in the electron spectral function as a result of edge reconstruction. It is clear that these features are associated with the redistribution of the weight of the original edge

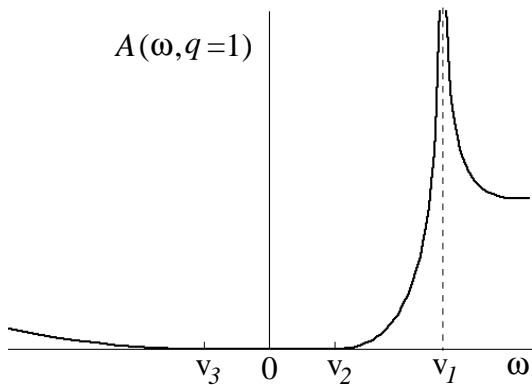


FIG. 2: The electron spectral function in the reconstructed edge has singularities on the lines $\omega = v_i q$ that correspond to the edge excitation modes. The singularity at $\omega = v_1 q$ is a divergence, and is the remnant of the δ -peak in the unreconstructed edge. The spectral function vanishes for $v_3 q < \omega < v_2 q$ (e.g. for $q > 0$) due to kinematic constraints. Shown is the case of the filling fraction $\nu = 1/3$.

mode. Therefore, one should look for an experiment in which the observed quantity is most closely related to the spectral function itself and not its integral over ω or q . Such a situation is realized in the so-called momentum-resolved tunneling experiments.^{7,8} In these experiments, the electron tunneling into the edge occurs across a barrier which is extended and homogeneous along the edge of the FQHE system, and so the electron's momentum along the edge is conserved. In what follows, we consider the simplest possible case of tunneling from the (non-reconstructed) edge of the QHE at the filling fraction $\nu = 1$ which is parallel to the reconstructed edge. The spectral function of the unreconstructed $\nu = 1$ edge is just a δ -function. This serves best to reveal the features of the spectral function of the reconstructed edge.

The setup and the structure of energy levels under these conditions are shown in Fig. 3. The energy E of the states is plotted as a function of momentum k along the two parallel edges. The two straight lines in plot b) correspond to single electron dispersion on the two sides of the barrier. Near the intersection point of these lines, the states on the left and on the right begin to mix, and tunneling becomes possible. We shall treat tunneling using Fermi golden rule. Finally, we neglect the interaction between the edge modes on the opposite sides of the barrier, while the intra-edge interactions are taken into account by strong renormalization of the (charged) mode velocities.

In what follows, we shall consider separately two cases: $m = 1$ and $m = 3$. For energetic reasons, the edge of the QH state with higher m is more susceptible to reconstruction,⁴ however, the changes in the spectral function are more noticeable for lower m .

There are two parameters that one can control: bias voltage V and magnetic field B . These two parameters are directly related to the structure of the spectrum: eV

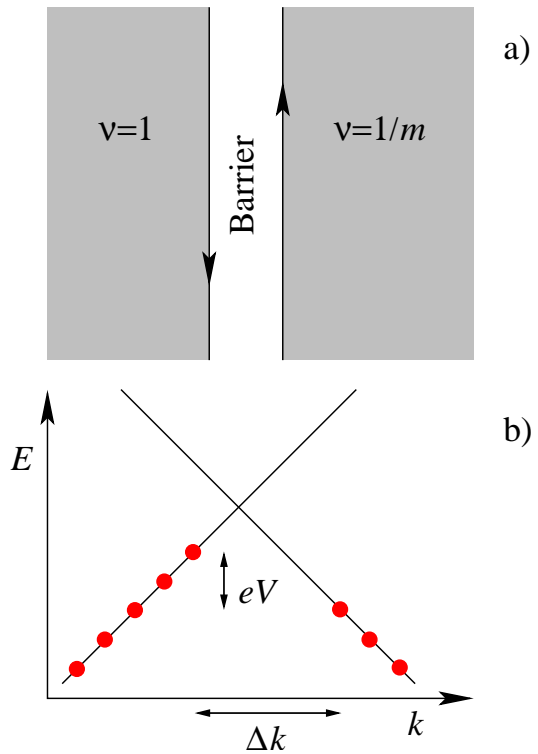


FIG. 3: a) The setup consists of $\nu = 1$ and reconstructed $\nu = 1/m$ states separated by a barrier which is uniform along the edges; b) The structure of the energy dispersion in the vicinity of the barrier (see text for details).

sets the difference between the Fermi energies on the two sides of the barrier, while the difference between the two Fermi momenta $\Delta k \propto B - B_0$, where B_0 is the strength of the magnetic field at which, in the absence of bias, the Fermi energy lies exactly at the dispersion lines crossing point. Below, we shall rescale B so that $\Delta k = B - B_0$.

Within our approximation, the tunneling current is given by the Fermi golden rule:

$$I(V, B) \propto \int A_1(\omega_1, q_1) A_2(\omega_2, q_2) [f(\omega_1) - f(\omega_2)] \times \delta(eV + \omega_1 - \omega_2) \delta(B - B_0 - q_1 - q_2). \quad (9)$$

Here, $A_1 = \delta(\omega - v_F q)$ is the spectral function of the $\nu = 1$ edge with the Fermi velocity v_F , and A_2 is the spectral function in Eq. (8); $f(\omega)$ is the Fermi distribution step function.

The result of the numerical evaluation of the differential conductance dI/dV as a function of V and $B - B_0$ is shown in Fig. 4. In general, the plot of $dI(V, B)/dV$ is very similar, but not identical to $A(\omega, q)$. In particular, both have 3 lines of singularities (marked by letters $L_{1,2,3}$ on the figure), one of them being a divergence. These lines correspond to the three edge excitation modes $\omega = v_i q$. Moreover, in the bow-tie region between L_2 and L_3 the differential conductance (as well as the current itself) is exactly zero. The reason for this

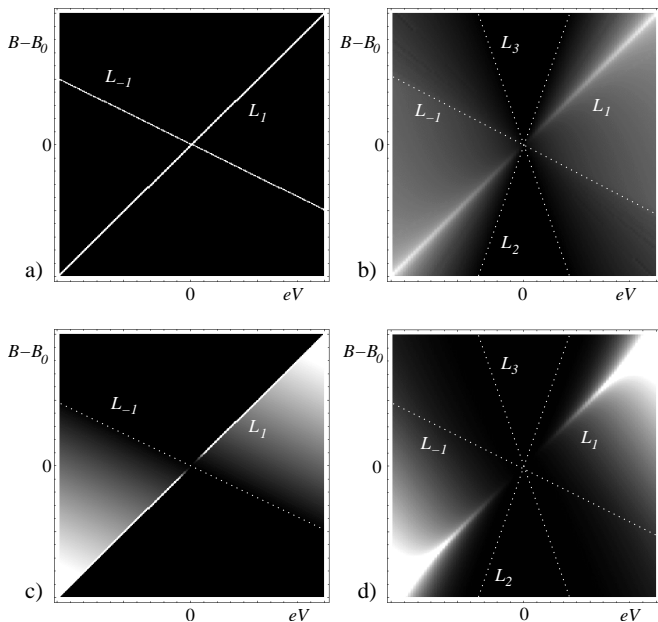


FIG. 4: Differential conductance dI/dV as a function of bias voltage V and magnetic field B for momentum-resolved tunneling from unreconstructed $\nu = 1$ edge to: a) unreconstructed $\nu = 1$ edge; b) reconstructed $\nu = 1$ edge; c) unreconstructed $\nu = 1/3$ edge; d) reconstructed $\nu = 1/3$ edge. Plotted is the derivative of the result in Eq. (9). Parameters are: $v_1 = 1$, $v_{2,3} = \pm 1/3$, $v_F = 2$, $\alpha_1 = m = \nu^{-1}$, $\alpha_{2,3} = 0.5$. The dashed lines are guides to the eye and are defined as $L_{1,2,3} = \{eV = v_{1,2,3}(B - B_0)\}$, $L_{-1} = \{eV = -v_F(B - B_0)\}$. See text for details.

is purely kinematic: In the region below the dispersion line of the slowest excitation in the system, one cannot satisfy the conservation of energy and momentum in tunneling. This is best visible if one plots dI/dV in a sweep of V at fixed B . The resulting plot is very similar to that of the spectral function in Fig. 2. In the situation, where reconstruction produces multiple edges, this kinematic constraint dictates that $dI/dV = 0$ in the region set by the two *slowest* velocities in the system.

We would like to point out, that while the singularities that correspond to the new neutral modes are rather weak and thus are difficult to observe, the general structure of the spectral weight transfer provides a clear indication of the edge reconstruction. In particular, in the bow-tie regions between L_1 and L_2 , and between L_3 and L_{-1} , dI/dV is zero before reconstruction and finite after. We note, that the rise of dI/dV in the region between L_3 and L_{-1} is due to the appearance of a (neutral) edge mode that propagates in the direction opposite to the direction of the original edge mode.

Although we have concentrated on the case of edge reconstruction described by a single point k_0 , the preceding discussion remains generally valid for multiple edge reconstruction as well. In that case, new lines of singu-

larities appear, while L_2 and L_3 correspond to the two slowest excitation modes.

One can't fail to notice that edge reconstruction leads to strong asymmetry in differential conductance, by suppressing a singularity on L_{-1} . This asymmetry is due to the fact that it is much easier to tunnel from the Fermi liquid, which describes the $\nu = 1$ edge, than from the non-Fermi liquid, which describes the reconstructed edge (this is true even for unreconstructed $\nu \neq 1$ edge, plot c) in Fig. 4, but in the case of $\nu = 1$ it is the reconstruction that produces the non-Fermi liquid at the edge). In order to understand this, let us consider the simplest case of Fermi liquid to non-Fermi liquid tunneling, namely from $\nu = 1$ to $\nu = 1/3$ (with no edge reconstruction in either edge; this corresponds to plot c) in Fig. 4). Plugging electron spectral functions in the two edges $A_1 = \delta(\omega - v_F q)$, $A_2 = |q|^2 \delta(\omega - v_1 q)$ into Eq. (9), we get a result in closed analytic form:

$$I \propto (v_F B + eV)^2 [\theta(v_F \Delta k + eV) - \theta(v_1 \Delta k - eV)], \quad (10)$$

where $\Delta k = B - B_0$. Differentiation with respect to V produces only one δ -function that comes from differentiating the second θ -function, while the derivative of the first θ -function is nullified by the prefactor. Physically, this nullification comes from the (non-Fermi liquid like) suppression of the electron spectral function in the $\nu = 1/3$ edge at low energies.

Finally, we would like to comment on the role of the omitted $n \neq 0$ terms in Eq. (5). Apart from the factors $\exp ink_0 x$, which trivially shift the momentum argument of the electron spectral function by nk_0 , all terms with $n \neq 0$ are qualitatively similar to the $n = 0$ term. Each of them produces a contribution to the Green's function which is of the form Eq. (6), albeit with larger exponents α_i . For that reason, all these terms make progressively less visible (but not necessarily unobservable) contributions to the spectral function.

Summarizing, we find that that edge reconstruction qualitatively changes the electron spectral function at the edge. The weight of the original sharp peak undergoes broad redistribution and the new edge modes that appear after the reconstruction show up as lines of singularities in the electron spectral function. We also suggest a momentum-resolved tunneling experiment which is best suited for probing the predicted features. We find that some of these features can be used to infer edge reconstruction. Perhaps, the most striking effect is expected in the reconstruction of the $\nu = 1$ edge. In this case, the emergent non-Fermi liquid character of the edge is expected to lead to strong asymmetry in the differential tunneling conductance.

We thank Matt Grayson and Leon Balents for helpful discussions. This work was supported by NSF grant No. DMR-0225698.

-
- ¹ X.-G. Wen, *Int. J. Mod. Phys. B* **6**, 1711 (1992).
- ² A. H. MacDonald, S. R. E. Yang, and M. D. Johnson, *Aus. J. Phys.* **46**, 345 (1993).
- ³ C. Chamon and X.-G. Wen, *Phys. Rev. B* **49**, 8227 (1994).
- ⁴ X. Wan, K. Yang, and E. H. Rezayi, *Phys. Rev. Lett.* **88**, 056802 (2002).
- ⁵ X. Wan, E. H. Rezayi, and K. Yang, *Phys. Rev. B* **68**, 125307 (2003).
- ⁶ K. Yang, *Phys. Rev. Lett.* **91**, 036802 (2003).
- ⁷ W. Kang et al., *Nature* **403**, 59 (2000); I. Yang et al., *Phys. Rev. Lett.* **92**, 056802 (2004).
- ⁸ M. Huber et al., cond-mat/0309221; work in preparation.
- ⁹ U. Zülicke, E. Shimshoni, and M. Governale, *Phys. Rev. B* **65**, 241315(R) (2002).
- ¹⁰ O. Heinonen and S. Eggert, *Phys. Rev. Lett.* **77**, 358 (1996).
- ¹¹ D. Carpentier, C. Peça, and L. Balents, *Phys. Rev. B* **66**, 153304 (2002).